Magnetosheath variations during the storm main phase on 20 November 2003: Evidence for solar wind density control of energy transfer to the magnetosphere

R. Kataoka,[1,2] D. H. Fairfield,[1] D. G. Sibeck,[1] L. Rastätter,[1] M.-C. Fok,[1] T. Nagatsuma,[2] and Y. Ebihara[3]

Received 26 August 2005; revised 4 October 2005; accepted 12 October 2005; published 15 November 2005.

[1] Energy transfer from the solar wind into the magnetosphere and ionosphere is controlled by the southward magnetic field in the magnetosheath which under normal high Mach number conditions is about four times the solar wind southward field. In a low Mach number regime, however, the magnetosheath compression is diminished by a low solar wind density when the magnetic field remains steady. When magnetic clouds with extremely strong magnetic field cause severe geomagnetic storms under such low Mach number conditions, the density control of the energy transfer is expected to be important in understanding ring current evolution. Here we show evidence for such a density effect using in-situ observation by the GOES and Cluster spacecraft in the magnetosheath during the main phase of the super storm on 20 November 2003. Results from a global magnetohydrodynamic (MHD) simulation with an embedded ring current model also support this density effect. **Citation:** Kataoka, R., D. H. Fairfield, D. G. Sibeck, L. Rastätter, M.-C. Fok, T. Nagatsuma, and Y. Ebihara (2005), Magnetosheath variations during the storm main phase on 20 November 2003: Evidence for solar wind density control of energy transfer to the magnetosphere, *Geophys. Res. Lett.*, *32*, L21108, doi:10.1029/2005GL024495.

1. Introduction

[2] The energy transfer from the solar wind into the Earth's magnetosphere and ionosphere is well known to be controlled largely by the strength of the southward interplanetary magnetic field (IMF) and the solar wind speed [*Akasofu*, 1981]. In reality it is the southward magnetosheath magnetic field that controls this energy transfer, but this field is normally directly related to the IMF when it is compressed by a relatively steady factor of about 4 during passage through a strong bow shock with Mach number more than 5. However, under low Mach number conditions, when Mach number M varies from 1 to 5, the compression ratio R changes from 1 to 4, according to a simple gas dynamic approximation by *Spreiter et al.* [1966], $R = (\gamma + 1)M^2/((\gamma - 1)M^2 + 2)$, where γ is the specific heat ratio. Recently, *Lopez et al.* [2004] pointed out that strong southward IMF conditions prevalent during magnetic storms can lower the Mach number to the point where the density controls the Mach number and hence the compression ratio. This variably compressed field controlled by the density can affect the energy transfer and the transpolar potential.

[3] Large geomagnetic storms are frequently driven by magnetic clouds which are characterized by low temperature plasmas with strong and smoothly rotating magnetic field [*Burlaga et al.*, 1981]. Within a magnetic cloud, the Alfvén Mach number is usually lower than average because the magnetic field is stronger than average while the solar wind speeds and densities tend to have typical values. The Alfvén Mach number generally has a value similar to the magnetosonic Mach number within the magnetic cloud because of the extremely low temperatures. Since the variations of magnetic field strength and solar wind speed are gradual while the density variations are somewhat irregular in typical magnetic clouds [*Lepping et al.*, 2003], it is expected that the importance of the density effect can be best evaluated in storms driven by magnetic clouds. In other words, the density should modulate the energy transfer due to the interaction between magnetic clouds and the bow shock.

[4] On 20 November 2003, the largest geomagnetic storm during solar cycle 23 was observed with the minimum Dst index of −472 nT. The solar wind cause was a magnetic cloud with the largest southward IMF observed during solar cycle 23 [*Gopalswamy et al.*, 2005]. This extremely large southward IMF also caused extremely reduced size of the magnetopause so that the GOES satellites in geosynchronous orbit observed the magnetic field of the magnetosheath during the storm main phase. The Cluster spacecraft simultaneously observed plasma parameters within the dusk magnetosheath. The magnetic cloud itself is in a low Mach number regime with small variations of the IMF and the solar wind speed and with a large density enhancement, thus providing an excellent opportunity to investigate the density effect.

[5] There are two reasons for the enhanced ring current energy density during this super storm. First, the flux of ring current ions may be enhanced due to high plasma sheet densities, as discussed for this particular superstorm in detail by *Ebihara et al.* [2005]. Secondly, enhanced convection electric fields may increase ring current ion energies. This paper advocates the second cause via the enhancement of the transpolar potential, and it is expected that the enhancement of the transpolar potential due to the density enhancement can be significant to the evolution of

[1]NASA Goddard Space Flight Center, Greenbelt, Maryland, USA.
[2]National Institute of Information and Communications Technology, Koganei, Tokyo, Japan.
[3]National Institute of Polar Research, Itabashi, Tokyo, Japan.

0094-8276/05/2005GL024495

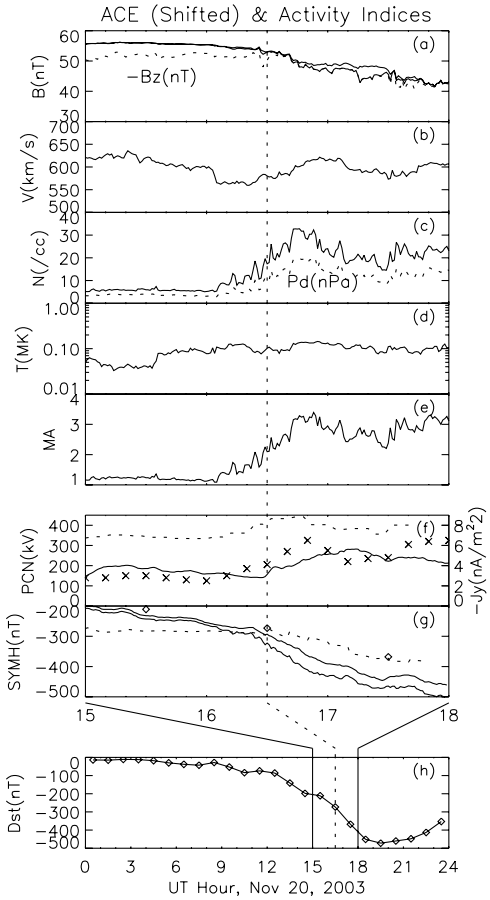

Figure 1. Solar wind parameters and geomagnetic activity indices during the main phase of the super storm on 20 November 2003. Solid lines are (a) the IMF strengths with and without the X component, (b) solar wind speed, (c) densities, (d) temperatures, (e) Alfvén Mach number, (f) northern hemispheric polar cap index, (g) SYM-H index, and (h) Dst index. Dotted lines are (a) the strength of the southward IMF in GSM coordinate system, (c) dynamic pressure, (f) transpolar potential obtained from the MHD simulation, and (g) SYM-H index obtained from the ring current model. Maximum strengths of Region 1 dynamo current density (see text in detail) are shown as crosses in panel (f). Diamonds in panels (g) and (h) shows the Dst index.

the ring current. The purpose of this paper is to report evidence for the density effect, focusing on the main phase of this super storm. A magnetohydrodynamic (MHD) simulation is conducted in an attempt to reproduce the magnetosheath observations by GOES and Cluster spacecraft. A ring current model is included to describe a realistic ring current evolution.

2. Simulation Models

[6] We use the Block Adaptive Tree Solar-wind Roe Upwind Scheme (BATSRUS) code to solve 3D MHD equations in a finite volume form using numerical methods related to Roe's Approximate Riemann Solver [*Powell et al.*, 1999]. The magnetospheric MHD part is attached to an ionospheric potential solver that provides electric potentials and conductivities in the ionosphere from magnetospheric field-aligned currents. The Earth's magnetic field is approximated by a dipole with a continually updated axis orientation and co-rotating inner magnetospheric plasma. The simulation box used in this study extends from −228 to 60 R_E in the X direction, and from −96 to 96 R_E in the Y and Z direction in the GSM coordinate system. ACE Level 2 data is propagated from the ACE position to the simulation inflow boundary at X = 60 R_E with two-hour running averaged velocity in the X component. Before input, the 64 sec plasma moment data are linearly interpolated on a 16 sec temporal grid of the magnetic field observations. For simplicity, the Bx component is ignored in this MHD simulation. We confirmed that the results exhibit little changes even if we include the Bx component, because of its relatively small amplitude as shown in the Section 3.

[7] The ring current is simultaneously simulated using a ring current model developed by *Fok et al.* [1996]. The temporal and spatial variations of the phase space densities are determined for the protons in the energy range from 1 to 300 keV. Magnetospheric protons are lost by two processes; charge exchange with neutral hydrogen and adiabatic loss cone. The simulation box is specified as between the magnetopause and the nightside boundary at 10 R_E. The magnetic field geometry inside the magnetopause, temperatures and densities at outer boundary, and the ionospheric potential distributions are obtained as the input parameters from the MHD simulation at each time step.

3. Model-Data Comparison

[8] The evolution of the Dst index on 20 November 2003 is shown in Figure 1h. The 3 hour time interval focused on in this paper is indicated by vertical solid lines, where the main phase is evolving toward its maximum depression. Other activity indices, the SYM-H and PCN indices, are plotted in Figures 1f and 1g enlarging the 3 hour period. The two solid lines in Figure 1g show (upper) the SYM-H and (lower) pressure corrected SYM-H [*Gonzalez et al.*, 1994]. As indicated by Dst and SYM-H, the strength of the ring current increases slowly and rapidly before and after 1630 UT, respectively. The empirical relation of *Trochichev et al.* [1996] is used to convert the PCN index into kV units to approximately represent the transpolar potential.

[9] Some input parameters for the MHD simulation are selected and compiled in Figures 1a–1e. In order to make it easier to compare with the ground-based activity indices in Figures 1f and 1g, input parameters are shifted by 10 min, where 10 min is a rough propagation time from 60 R_E to the Earth with a 600 km/sec speed. The strength of the dominant southward IMF gradually decreases after 1630 UT, and there exist only minor B_Y (B_X) components before (after) this time. This 3 hour time interval is a part of the magnetic cloud, identified by a strong magnetic field with a smooth rotation [see *Gopalswamy et al.*, 2005].

[10] As shown in Figure 1e, the 3 hour time interval is under a low Mach number condition of $M_A < 4.0$. Before 1630 UT, an extremely low M_A condition of $M_A < 2.0$ creates an extremely weak bow shock and minimal field compression according to the Rankine-Hugoniot theory. It is noteworthy here that the subsolar bow shock

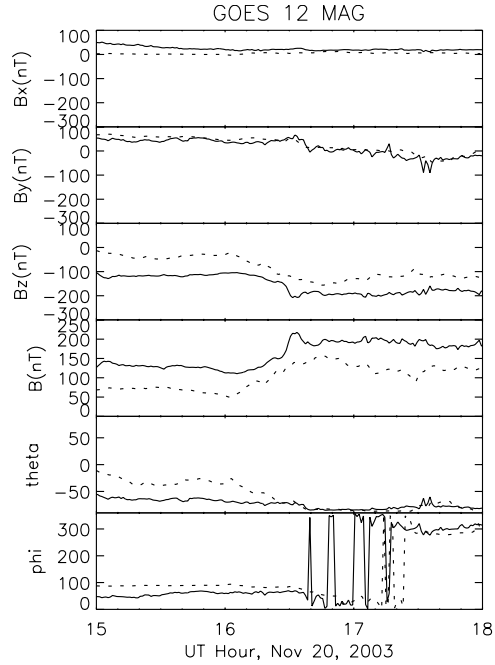

Figure 2. Magnetic fields observed by the GOES 12 satellite (solid lines) in GSM Cartesian (Bx, By, Bz) and polar (B, θ, φ) coordinate systems. Dotted lines show the prediction from the MHD simulation.

expands up to X = 35 R_E in the MHD simulation as has been typically observed under such extreme conditions [e.g., *Fairfield et al.*, 2001]. After 1630 UT, a large enhancement of the solar wind density causes a condition of $M_A > 2.0$, and the compression ratio across the bow shock increases to larger value. The PCN index in Figure 1f tracks the first order trend of the Mach number variations.

[11] Figure 2 compares the magnetic field observation (solid lines) by GOES 12 around noon with the simulation results (dotted lines). GOES 12 was completely within the magnetosheath as indicated by the southward magnetic field during this entire time interval. The variation of the magnetic fields is reasonably reproduced by the MHD simulation. Some disagreements are found only in the magnetic field amplitudes and transient features. What we can learn from this comparison is that, even if the IMF strength is somewhat steady as shown in Figure 1a, the magnetosheath magnetic field is highly variable due to the density effect under low Mach number conditions. It is also worthwhile noting that GOES 10 at prenoon sector experienced the magnetopause crossing at 1630 UT, exactly the same time as predicted by the MHD simulation (not shown).

[12] Figure 3 compares the Cluster observations (solid lines) and the simulation results (dotted lines). Four sec resolution FGM and CIS-HIA moment data from Cluster 1 are shown as representative of the other Cluster spacecraft. These spacecraft are close to the dusk magnetopause and they observe a relatively slow plasma flow associated with the boundary layer from 1515 to 1616 UT. Outside of this interval when Cluster is in the magnetosheath, the traces show reasonable agreement indicating that the simulation reproduces the magnetosheath data quite well. Understanding the cause of the relatively weak magnetosheath magnetic field in the MHD simulation is beyond the scope of this paper, but this discrepancy does not change the conclusions of the paper.

4. Discussion and Conclusion

[13] After 1630 UT, the averaged decrease rate of SYM-H is about 1.5 times larger than that of before 1630 UT; about −100 nT (−150 nT) per 1.5 hours before (after) 1630 UT. The dotted line in Figure 1g shows the simulated SYM-H index derived from an equation using the total energy of trapped particles [*Ebihara et al.*, 2005] obtained from the ring current simulation. A similar trend is found in the simulated SYM-H, while the ring current strength is smaller than that of the observed SYM-H. The dotted line in Figure 1f shows the transpolar potential drop obtained from the MHD simulation, which is also used for the input to the ring current simulation. Since there is a significant offset of ∼150 kV in the transpolar potential obtained from the MHD simulation because of small ionospheric conductivities in the MHD simulation, we only focus on the relative enhancement of ∼100 kV after 1630 UT, which is similar to the PCN observation. Consistent with the variations of the PCN and SYM-H indices, all of the results from the ring current simulation suggest that

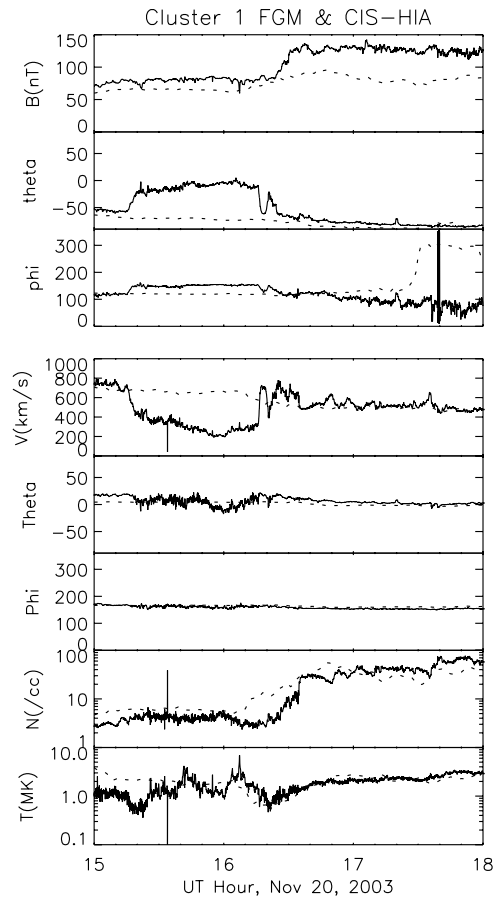

Figure 3. Magnetic fields and plasma moments observed by the Cluster 1 satellite (solid lines). From top to bottom, shown are magnetic fields and ion velocities in GSM polar coordinate system, ion number density, and ion temperature. Dotted lines show the prediction from the MHD simulation.

the enhanced magnetospheric convection, which is approximately proportional to the enhanced transpolar potential drop, pushes the protons from the nightside plasma sheet deeper into the inner magnetosphere, resulting in the enhanced ring current.

[14] Here we discuss the connection between the density effect and the enhancement of the transpolar potential drop. Due to the prolonged strong southward IMF, the whole time interval from 1500 to 1800 UT is in a state of so-called "transpolar potential saturation" [see *Hairston et al.*, 2005]. The expression for the saturation potential presented by *Siscoe et al.* [2002] depends on the solar wind density, with higher densities leading to larger saturation potentials. However, it may not be appropriate to simply apply their expression in this case study because the expression does not take into account the low Mach number conditions with highly variable magnetosheath compression ratios seen on this day. Under the saturated conditions, the Region 1 current system usurps the role of the Chapman-Ferraro current system to maintain pressure balance at the magnetopause via the JxB force [*Siscoe et al.*, 2002]. The dynamo region of the Region 1 current system is located on the poleward side of the cusp, where the diamagnetic current flows in the dusk-to-dawn direction, opposing the local electric field [*Tanaka*, 2000]. In the X-Z plane in the northern hemisphere, the electric current in the negative Y direction approximately represents the diamagnetic current because of nearly southward geomagnetic field and nearly sunward gradient of the thermal pressure. The cross symbols in Figure 1f show the maximum strength of the negative J_Y obtained from the MHD simulation in the X-Z plane within the dynamo region in the northern hemisphere. Note that the variation of the maximum diamagnetic current is approximately proportional to the variation of transpolar potential drop.

[15] Such a good correlation between the diamagnetic current and polar cap potential is interpreted based on the MHD simulation results. The strength of the diamagnetic current is largely controlled by the thermal pressure of the cusp. When the magnetic field in the magnetosheath is enhanced due to the density effect, the magnetosheath density itself is also similarly enhanced via the compression at the bow shock. Via magnetopause reconnection, stronger southward magnetosheath magnetic fields provide larger transfer rate for the dense magnetosheath plasma into the cusp to enhance the cusp pressure. One can expect that the diamagnetic current is proportional to the transpolar potential via the simplest current-circuit view of the Region 1 current system because the MHD simulation results show that there are relatively weak variations of the electric field in the dynamo region and the ionospheric Pederson conductivity. Therefore it is concluded that the density effect is connected to the transpolar potential via the dynamo current associated with the high-pressure cusp structure maintained by the coexistence of dense plasma and strong southward magnetic field in the magnetosheath.

[16] This is the first paper showing evidence that the density control of the magnetosheath field due to Mach number changes is important for ring current evolution; under relatively steady southward IMF with variable densities, the ring current strength increases with densities at the same time. The results obtained imply that the density effect becomes more important in magnetic clouds with stronger magnetic field where the Mach number is more apt to be small. Also, the results imply that the magnetic clouds with higher density are more geoeffective for similar values of southward IMF, and the density distribution within the magnetic cloud is important to control storm evolutions.

[17] **Acknowledgments.** We appreciate valuable discussions on the property of magnetic clouds with Ron Lepping and Len Burlaga. We acknowledge Henri Rème for his helpful support on Cluster CIS data. We thank Aaron Ridley and Gabor Toth for their valuable comments about the MHD code. The MHD and ring current simulations are operated by CCMC. ACE, Cluster, and GOES data are provided by CDAWeb. We thank the DMI for providing the PCN index. The Dst and SYM-H indices are provided by WDC-C2, Kyoto University. R. K. is supported by a research fellowship of the Japan Society for the Promotion of Science for Young Scientists.

References

Akasofu, S. (1981), Energy coupling between the solar wind and the magnetosphere, *Space Sci. Rev.*, *28*, 121.

Burlaga, L. F., et al. (1981), Magnetic loop behind an interplanetary shock: Voyager, Helios and IMP-8 observations, *J. Geophys. Res.*, *86*, 6673.

Ebihara, Y., et al. (2005), Ring current and the magnetosphere-ionosphere coupling during the superstorm of 20 November 2003, *J. Geophys. Res.*, *110*, A09S22, doi:10.1029/2004JA010924.

Fairfield, D. F., et al. (2001), The location of low Mach number bow shocks at Earth, *J. Geophys. Res.*, *106*, 25,361.

Fok, M.-C., et al. (1996), Ring current development during storm main phase, *J. Geophys. Res.*, *101*, 15,311.

Gonzalez, W. D., et al. (1994), What is a geomagnetic storm?, *J. Geophys. Res.*, *99*, 5771.

Gopalswamy, N., et al. (2005), Solar source of the largest geomagnetic storm of cycle 23, *Geophys. Res. Lett.*, *32*, L12S09, doi:10.1029/2004GL021639.

Hairston, M. R., et al. (2005), Saturation of the ionospheric polar cap potential during the October–November 2003 superstorms, *J. Geophys. Res.*, *110*, A09S26, doi:10.1029/2004JA010864.

Lepping, R. P., et al. (2003), Profile of an average magnetic cloud at 1 AU for the quiet solar phase: Wind observations, *Sol. Phys.*, *212*, 425.

Lopez, R. E., et al. (2004), Solar wind density control of energy transfer to the magnetosphere, *Geophys. Res. Lett.*, *31*, L08804, doi:10.1029/2003GL018780.

Powell, K. G., et al. (1999), A solution-adaptive upwind scheme for ideal magnetohydrodynamics, *J. Comput. Phys.*, *154*, 284.

Siscoe, G. L., et al. (2002), Transpolar potential saturation: Roles of region 1 current system and solar wind ram pressure, *J. Geophys. Res.*, *107*(A10), 1321, doi:10.1029/2001JA009176.

Spreiter, J. R., et al. (1966), Hydromagnetic flow around the magnetopause, *Planet. Space Sci.*, *14*, 223.

Tanaka, T. (2000), Field-aligned-current systems in the numerically simulated magnetosphere, in *Magnetospheric Current Systems*, *Geophys. Monogr. Ser.*, vol. 118, edited by S. Ohtani et al., p. 53, AGU, Washington, D. C.

Trochichev, O., et al. (1996), Cross polar cap diameter and voltage as a function of PC index and interplanetary quantities, *J. Geophys. Res.*, *101*, 13,429.

Y. Ebihara, National Institute of Polar Research, Itabashi, Tokyo, Japan.

D. H. Fairfield, M.-C. Fok, L. Rastätter, and D. G. Sibeck, NASA, Goddard Space Flight Center, Laboratory for Extraterrestrial Physics, Code 695, Greenbelt, MD 20771, USA.

R. Kataoka and T. Nagatsuma, National Institute of Information and Communications Technology, Koganei, Tokyo, Japan. (ryuho@nict.go.jp)